

# THE NATURE OF SPREAD- $F$ IRREGULARITIES IN ANTARCTICA

By G. G. BOWMAN\*

[Manuscript received June 6, 1968]

## *Summary*

Some characteristics of spread- $F$  ionograms from the Antarctic region are discussed. Very disturbed periods, such as when magnetic storms are in progress, have been neglected in this analysis. Two important characteristics are the frequent occurrence of resolved as well as diffuse traces, and the appearance from time to time of an enhanced trace which seems to be produced by signals that arrive from directions close to the magnetic field direction. Two independent sets of spread- $F$  traces are reported. Several possible models are examined and some ray tracing performed. The analysis favours a model that incorporates kinking of the contours of equal ionization density to produce "wavelengths" in the ionospheric structure of some tens of kilometres. Because of the similarities at mid and high latitude regions, it is suggested that similar mechanisms are operating at both regions to produce spread- $F$ .

## I. INTRODUCTION

The precise nature of the irregularities responsible for spread- $F$  signals has concerned workers in the field for many years. For mid and high latitude regions the most favoured theory in the past has been one that regarded the irregularities as relatively small-scale columns of enhanced ionization lying along the direction of the magnetic field. Calculated dimensions for these irregularities are of the order of 1 km (Yeh and Swenson 1964). Signals scattered from such irregularities should produce a diffuse record. Since a significant percentage of mid and high latitude ionograms show spread- $F$  as diffuse echoes, this appeared to be a satisfactory model. In a recent summary article on spread- $F$ , Herman (1966) discusses this and other theories.

Results by Klemperer (1963) appear significant because they show that high latitude spread- $F$  signals have a high specular component, which does not support the scattering theory. Some of the more recent work has suggested various waveguide mechanisms. For example, perhaps signals that propagate in a waveguide mode between field-aligned columns of enhanced ionization are responsible for spread- $F$  (Booker 1961; Pitteway 1962); or perhaps these extra traces on ionograms result from waveguide propagation between field-aligned sheets of ionization, as has been suggested for some topside reflections (Muldrew 1963).

In the present paper the nature of the spread- $F$  irregularities over a high latitude region (Antarctica) is considered. This follows an examination of many ionograms from this region which show the phenomenon. Several aspects of the phenomenon will be illustrated and discussed in Section II. Any theory that attempts to describe the nature of these irregularities must be consistent with the experimental observations treated in Section II.

\* On leave to Space Systems Division, AVCO Corporation, Lowell, Massachusetts, U.S.A., from present address: Department of Physics, University of Queensland, St. Lucia, Brisbane, Qld. 4067.

It must be stressed that the appearance of ionograms in Antarctica, when additional echoes (spread- $F$  echoes) are present, can show a variety of forms. The reason for this seems to be the dynamic character of the ionosphere in this region. Topside soundings by artificial Earth satellites (Warren 1963; Sharp, Crother, and Gilbreth 1964; Titheridge 1966) show that the electron density distribution in high latitude regions can change radically as the satellite moves from one place to another. Because of this, and the fact that the direction of arrival of spread- $F$  signals can be off-vertical by as much as  $60^\circ$  (Bowman 1968a), it is not surprising that relatively large-scale disturbances, which affect the background ionization distribution, can produce additional complications in the appearance of the traces from the spread- $F$  irregularities.

During times of magnetic storms, apart from blackout conditions, drastic changes can occur in the electron density profile of the  $F_2$  layer. Additional low-lying ionization in the  $D$  and  $E$  regions is common at these times leading to further retardation effects, especially on the off-vertical traces that traverse these regions obliquely. The appearance of spread- $F$  traces at these times is considerably different from that at quiet times.

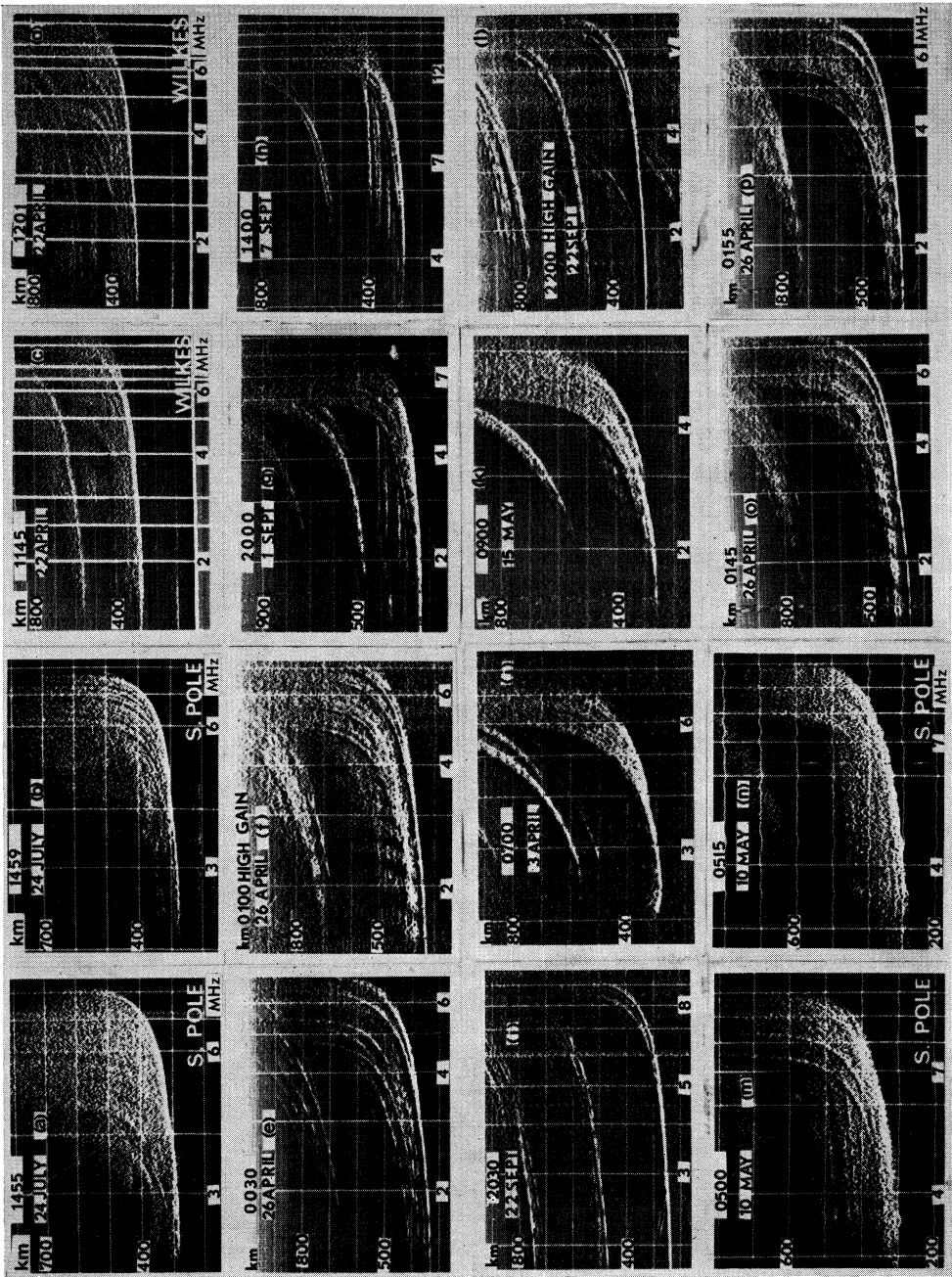
When all observable aspects of the phenomenon are considered, spread- $F$  traces can be seen in many different forms, more than can be illustrated or discussed adequately here. Contrast, for example, Figures 1(a), 1(d), and 1(f) for some idea of the differences in appearance that can occur. Therefore, the phenomenon of high latitude spread- $F$  cannot be represented by a single ionogram, or even by a restricted group of ionograms.

Although disturbances of some kind or other producing changes in the electron density distribution of the layer seem to be nearly always present, periods when pronounced changes occur, such as when magnetic storms are in progress, have been avoided in the present analysis. Only those aspects of the phenomenon that occur regularly and can be identified in an ionosphere that appears to have a relatively stable background will be considered. Multilayer conditions which occur in the daytime have also been neglected. Spread- $F$  conditions during the occurrence of large-scale disturbances require additional study. In any case, the presence of these large-scale disturbances only complicates attempts to decide upon the nature of the spread- $F$  irregularities.

In Section III a number of possible mechanisms are discussed and certain calculations made. When ray tracing through model ionospheres is performed, the effect of the magnetic field will be neglected. In view of the considerable differences in the nature of the various models that are proposed, this approximation seems justified. Its use cannot be expected to influence the choice of a particular model. It will be shown that some of these models are inconsistent with experimental observations. Discussion on, and conclusions from, this analysis are treated in Sections IV and V respectively.

---

Fig. 1.—A selection of ionograms showing spread- $F$  characteristics in Antarctica. Most of the records are from Ellsworth. The South Pole and Wilkes records are labelled. All records were taken in 1958 and local times are used.



In this paper the term "satellite" refers to the additional traces on ionograms which are satellites of the main trace. The term should not be taken as referring to information from orbiting Earth satellites. The subdivisions "range spreading" and "frequency spreading" of the spread- $F$  phenomenon are defined by Bowman (1960).

Some 25 station-months of ionosonde records taken during the equinoctial and winter months of sunspot-maximum years (1957–1958) have been examined for this analysis. In addition, 20 station-months for 1961 have also been inspected for the same periods of the year. The stations used were located in Antarctica and were: Ellsworth (dip  $66^\circ$ ), Byrd (dip  $75^\circ$ ), South Pole (dip  $75^\circ$ ), Little America (dip  $80^\circ$ ), and Wilkes (dip  $82^\circ$ ). Although the phenomena discussed in Section II are common to all stations, ionograms illustrating these effects are shown from only Ellsworth, South Pole, and Wilkes.

## II. SOME CHARACTERISTICS OF SPREAD- $F$ IONOGRAMS AT HIGH LATITUDES

In this section certain easily recognized characteristics of spread- $F$  ionograms that are recorded in the Antarctic region will be considered.

### (a) *Off-vertical Angles of Arrival*

Ionograms taken at the Ellsworth station show a system of nulls, equally spaced in frequency on certain sections of the main and satellite traces. The Ellsworth station is located on the Filchner iceshelf of the Antarctic continent at a geographic position several hundreds of kilometres outside the night-time auroral zone. The nulls result from the interference between the ray travelling upwards from the antenna and the ray that travels first to the bottom of the iceshelf before being reflected upwards. Because of the systematic shift with range of the frequency of the nulls for diffuse sporadic- $E$  reflections, it has been possible to calibrate the system so that the off-vertical angles of arrival of signals reflected from any level can be determined with reasonable accuracy. Bowman (1968a) has shown that when spread- $F$  traces are present, whether they be diffuse or resolved, the measured angles of arrival suggest that, at least for range spreading at the low frequency end of the ionograms, the satellite signals are reflected from approximately the same level as the signals at the same frequency that travel vertically to produce the main trace. The extra range of the traces produced by these signals is a consequence of the ray paths to and from the spread- $F$  irregularities being off-vertical. Figures 1(e) and 1(f) illustrate the shift in frequency of the nulls for spread- $F$  satellite traces. Even when a certain amount of the excess range appears to result from retardation effects, significant off-vertical angles are measured. This suggests that the reflection levels for all frequencies of the satellite traces are close to the reflection levels of the corresponding frequencies of the main trace. Klemperer (1963) has obtained results that indicate a semi-angle of  $13^\circ$  for the cone embracing the returning spread- $F$  signals. It is not known if these measurements apply to frequency spreading or range spreading. The iceshelf measurements show that when range spreading is present, irrespective of whether or not there is a spread in critical frequency, large off-vertical angles (up to  $60^\circ$ ) are common. These results would seem to be important when considering the nature of the spread- $F$  irregularities.

*(b) Diffuse and Resolved Traces*

One of the most striking aspects of high latitude spread-*F* traces is the fact that the spreading from the main trace in range and/or frequency on the ionogram often appears diffuse. However, what is probably of equal importance is that, on just as many occasions, structure is revealed in the form of resolved traces. Inspection of all the ionograms shown in Figure 1 shows the nature of the resolved traces that are often seen. On most of the occasions when structure is present only part of the ionogram is resolved while the rest of the ionogram is diffuse. However, ionograms can be found when the satellite traces are all resolved. The change from complete diffuseness to partial resolution (or vice versa) can occur over a short interval of time. Compare, for example, Figures 1(a) and 1(b) showing ionograms (from South Pole) taken 4 min apart. At 16 min later the ionogram appears diffuse again as in Figure 1(a). Compare also Figures 1(c) and 1(d) showing ionograms (from Wilkes) taken 16 min apart. Again in this case, 14 min later the ionogram is completely diffuse.

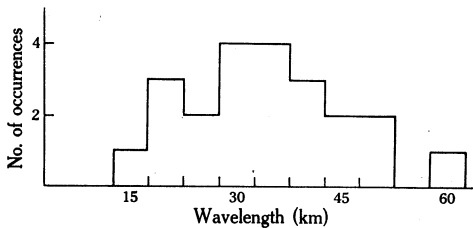


Fig. 2.—Distribution of irregularity spacings deduced from a small sample of Antarctic ionograms.

In both cases the first ionogram is almost completely diffuse and yet in several minutes changes to an ionogram that has a certain amount of structure. It does not seem likely that the nature of the irregularities changes over these small intervals of time to give different records. Thus the ionospheric structure that produces the resolved traces is, in all probability, also responsible for the diffuse traces. As relatively small height changes are always taking place for the  $F_2$  layer, it is possible that changes in the orientation of the background layer, relative to the horizontal plane, are effective in allowing structure to be seen more clearly at some times than at others. It seems important that both aspects (diffuseness and resolution) be considered when investigating models to explain Antarctic spread-*F*.

Using certain simplifying assumptions, estimates can be made of the horizontal spacings (wavelengths) between individual components of the irregularities that produce resolved range spreading. Figure 12 of Bowman (1968*a*) illustrates the method. Figure 2 in the present paper shows the distribution of wavelengths determined from a small sample of ionograms from Antarctica which showed satellite traces. Wavelengths of some tens of kilometres are found.

*(c) Two Sets of Satellite Traces*

Examination of the structure in Antarctic spread-*F* ionograms reveals that two independent sets of satellites can be recognized fairly frequently. The predominant set (set 1) consists of satellite traces which appear as replicas of the main trace, except that their critical frequencies are usually lower. A particular trace shows a smooth

change in curvature, free of kinks of any kind, over the range of frequencies it records. Figures 1(b), 1(e), and 1(f) show examples of set 1. The other set (set 2) consists of traces that have shapes showing less retardation effects than the main trace. The critical frequencies of these traces are obviously greater than that of the main trace, although the high frequency end of the traces is missing on most occasions. They can be distinguished from set 1 because they appear to cut across the traces of set 1 at a particular frequency range. They are seen up to ranges in excess of the main trace of several hundreds of kilometres and seem to favour occurrence at the higher ranges. Figure 3 illustrates the two sets. Set 1 is often present when set 2 is not. Figures 1(g) and 1(h) show examples where set 2 can be clearly distinguished from set 1. A careful inspection of the other ionograms of Figure 1 will show that even though it is sometimes difficult to distinguish between the two sets, they are nevertheless present quite often (see e.g. Fig. 1(k)). Figure 1(m) indicates that even when the ionograms show a certain degree of diffuseness, the two sets can sometimes be distinguished. Set 2 seems to be resolved more often than set 1. Another distinguishing feature between the sets is that set 1 can be seen on the higher traces (e.g. second- and third-hop traces) whereas this does not occur for set 2.

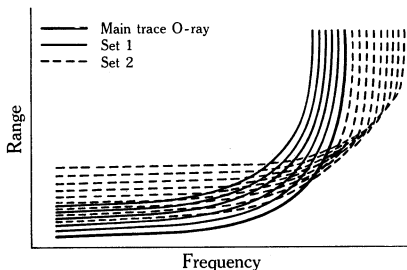


Fig. 3.—Illustration of two sets of spread- $F$  traces for the  $O$ -ray mode.

When the traces are resolved for set 1 there is a smooth progression between an increase in range at the low frequency end and a decrease in critical frequency for corresponding traces at the high frequency end. Direction-of-arrival information on spread- $F$  at Ellsworth (Bowman 1968a) has shown that the increase in range at low frequencies really represents an increase in off-vertical angle of the spread- $F$  signals. The fact that the shapes of the satellite traces of this set closely resemble the shape of the main trace suggests that, whatever forms the spread- $F$  irregularities take, they should be relatively simple distortions of the background ionization. In some cases, the discrete traces can be followed from high frequencies near the critical frequency to the frequency of the lower limit of the ionosonde indicating that, on these occasions, the individual irregularities can be identified from the lowest levels right up to the maximum of the  $F_2$  layer.

Any model that satisfies these observations must allow for a variation in the electron density distribution along various off-vertical paths, which is somewhat similar to the variation in the vertical direction; otherwise, trace shapes similar to the shape of the main trace would not be produced. It seems likely that the spread in frequency is produced by a horizontal gradient in  $f_0F_2$ . The  $f_0F_2$  value of the satellite traces would then change as signals with different off-vertical angles reach

the maximum of the layer at different horizontal displacements from the zenith position. It has been shown by Sato and Rourke (1964) that a positive gradient of  $f_0F_2$  exists in a direction towards the magnetic pole in Antarctica at night.

(d) *Enhanced Satellite Traces*

When the satellite traces are resolved, the high frequency end of the traces close to the critical frequency is often missing. Although this is pronounced for set 2, it is also true to a lesser degree for set 1. When the main trace can be distinguished from the satellite traces of the spread- $F$  phenomenon, it is often weak or missing for frequencies close to the critical frequency.

However, there is sometimes one particular trace among the satellite traces that appears to be produced by signals that are relatively strong at all frequencies right up to the critical frequency. At times this trace can be identified from an otherwise diffuse record because of its greater signal strength. At Ellsworth the measured off-vertical angle of arrival of this trace, from examples where the null system is well defined, is approximately  $24^\circ$ . This is consistent with a direction of arrival along or close to the magnetic field direction for this station, which has a magnetic inclination (dip) of  $66^\circ$ . If the range in excess of the main-trace range at the low frequency end is regarded as a true increase in range produced by the signal direction being off-vertical, then the observed enhanced traces at South Pole and Wilkes also suggest propagation close to the magnetic field direction. An enhanced trace from South Pole is illustrated by Figure 1(*m*). Enhanced traces for Ellsworth are shown in Figures 1(*e*), 1(*f*), and 1(*p*). It should be noted how well the critical frequencies of these traces are defined compared with the corresponding main-trace critical frequencies.

When ionograms are taken at 15 min intervals, it is unusual for two consecutive ionograms to show the enhanced trace. Figure 1(*m*) shows an ionogram with an enhanced trace prominent in an otherwise diffuse record. Five minutes previously (at 0455 hr) the record is almost completely diffuse as it is 15 min later (illustrated by Fig. 1(*n*)). Figures 1(*o*) and 1(*p*) show another pair of ionograms taken 10 min apart. The first shows no enhanced trace while it is clearly observable in the second record.

(e) *Low Frequency Retardation of Satellite Traces*

It might be thought when the satellite traces show a spread in frequency near the critical frequency of the main trace but not a spread in range at the lower frequencies (frequency spreading) that the irregularities are confined to the region of the  $F_2$  layer just below the maximum of ionization density. However, on some occasions when frequency spreading exists, the low-lying ionization in the  $D$  and/or  $E$  regions is large enough to produce retardation at the low frequency end of the  $X$ -ray trace which is greater than usual. Similar retardation effects are seen, although less frequently, for the  $O$ -ray trace. If the satellite traces that produce frequency spreading are off-vertical, they will suffer greater retardation effects than the main trace since the path through the retarding region is longer. This seems to be the case in the examples shown here (Figs. 1(*i*) and 1(*j*)) since the increased retardation of the

satellite traces at the low frequency end is sufficient to distinguish them from the main trace. Satellite traces are not observed at medium frequencies on the ionograms illustrated by Figures 1(i) and 1(j). Figure 1(i) shows a single satellite trace giving resolved frequency spreading near the critical frequency. The single satellite trace can also be seen near the *X*-ray "tail". Figure 1(j) shows unresolved frequency spreading near the critical frequency and resolved range spreading near the *O*-ray "tail". This aspect of frequency spreading suggests that the irregularities that produce these effects extend through the layer from the lowest levels up to at least the level of maximum electron density. The irregularities are not apparently confined to any particular region of the layer. In these cases, the real increase in range of the off-vertical satellite traces is probably not great enough for them to be observed at medium frequencies where retardation effects are at a minimum.

#### (f) *Spreading on Multiple-hop Traces*

During equinoctial months, there are occasions when the first-hop main trace is clear of satellite traces. However, when this occurs it does not necessarily mean that the multiple-hop traces (e.g. second- or third-hop trace) are also free of satellite traces. Figure 1(l) is an example of this aspect of the spread-*F* phenomenon. The range spreading present on the third trace consists of off-vertical signals. The displacement of nulls in Figure 1(l) gives 30°, 40°, and 43° respectively as the off-vertical angles of arrival of the three well-defined traces (Bowman 1968a). Also, this ionogram shows the tenth-, eleventh-, and twelfth-hop traces with some spreading associated with these traces. The positions of nulls on these high multiple traces indicate a vertical direction of arrival for their main traces. These results suggest that irregularities are present, but that they have certain features that prevent detection for one-hop reflections but allow it for multiple hops. A possible model is proposed in Section III(e).

#### (g) *Similarity to Mid Latitude Spread-F Traces*

The observations reported in the previous subsections deal with conditions when the ionosphere, although at times markedly disturbed by the spread-*F* irregularities, was nevertheless relatively free from the larger-scale disturbances. The results reported in this section are similar in nearly all respects to those reported by the author for a mid latitude station (Bowman 1960, 1968b).

Night-time *D*-region effects are negligible at mid latitudes so the observation of retardation effects at low frequencies for satellite traces (Subsection (e) above) is not made at mid latitudes. Also, set 2 of the satellite traces is not observed at mid latitudes. The observation of this set may be related to the slope of the magnetic field at a particular station. Apart from the ionograms illustrated in Figure 1 and the spread-*F* characteristics at high latitudes which are discussed in this section, the general impression gained as the Antarctic records were examined was that the phenomenon was the same at both latitudes. Of course, spread-*F* conditions, when the high latitude ionosphere is otherwise greatly disturbed by large-scale disturbances, have been disregarded for this assessment.

The enhanced trace (Subsection (*d*) above) which is so pronounced at the high latitude regions (Ellsworth, dip 66°; South Pole, dip 74°) has been reported by Bowman (1957, 1960) from Brisbane (dip 57°) and Townsville (dip 45°) for both *E*- and *F*-region reflections.

### III. SPREAD-*F* THEORIES FOR HIGH LATITUDE REGIONS

In this section a number of mechanisms or models that could possibly be responsible for the production of spread-*F* traces will be considered.

#### (*a*) *Scattering from Columns of Enhanced Ionization or Other Discontinuities*

As discussed in the Introduction, this seems to be ruled out as a possibility for high latitude regions following the measurement by Klemperer (1963) of a high specular component in spread-*F* echoes. In any case, the frequent appearance of resolved satellite traces on Antarctic spread-*F* ionograms is inconsistent with a scattering mechanism. Inspection of the various ionograms shown in Figure 1 suggests that relatively large ionospheric structures which give resolved traces under certain circumstances must be considered when spread-*F* models are being proposed.

#### (*b*) "Blobs" or "Holes" in the Background Electron Density Distribution

When spread-*F* is present, whether or not range spreading forms part of the phenomenon, the satellite traces will show a spread in critical frequency. It might be thought that measurement of the spread in critical frequency would give a measure of the increase or decrease over the background ionization of the electron density at the centre of the irregularities. In this case the irregularities would be regarded as having the form of "blobs" or "holes". The range of critical frequency  $\Delta f$  represents a change in electron density  $\Delta N$ , and so the proportional change in electron density  $\Delta N/N$  can be calculated. Here  $N$  represents the background electron density.

In frequency spreading, the spread-*F* signals seem to originate from near-vertical propagation because of the limited range spreading at these times. The background electron density distribution shown in Figure 4 has been derived from the main trace of the ionogram shown in Figure 1(*k*). An electron density profile, determined from this record by an  $N(h)$  analysis (Ventrice and Schmerling 1958) was subsequently adjusted empirically so that a calculation of the shape of the main trace from the profile produced a trace shape reasonably close to the observed main trace. Only the top portion of the electron density profile is shown in Figure 4. This figure also shows three localized irregularities in the electron density, (*a*) a hole, and (*b*) and (*c*) blobs. If the effect of the magnetic field is neglected, the group paths to various reflection levels can be calculated for vertical propagation along lines that pass through the centres of these irregularities by evaluating the integral

$$\int 1/\mu \, ds.$$

The refractive index is  $\mu$  and  $ds$  is the increment in the vertical path. These calculations can be used to derive satellite traces. The calculated satellite traces for the irregularities (*a*), (*b*), and (*c*) of Figure 4 are shown in Figures 5(*a*), 5(*b*), and 5(*c*) respectively.

The shapes of the satellite traces are noticeably different from that of the main trace as would be expected because the electron density profiles in a vertical direction through the irregularities are different from that of the undisturbed ionosphere. Observations on frequency spreading show that the satellite traces merge gradually with the main trace, but for these models the satellite traces come out of the main trace somewhat abruptly at a particular frequency.

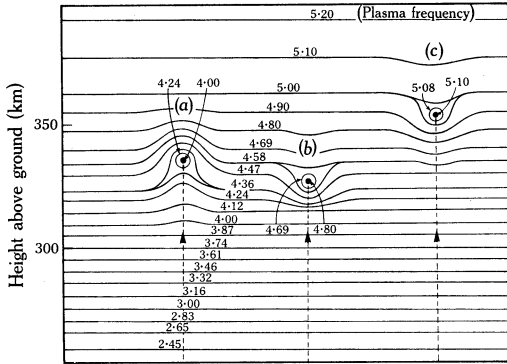


Fig. 4.—Model of spread-*F* irregularities incorporating localized enhancements and reductions in electron density concentration. All frequencies are in megahertz.

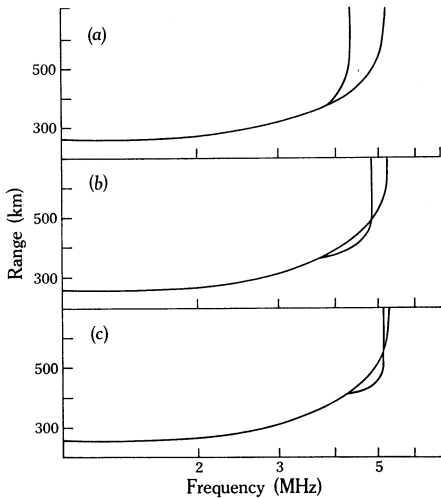


Fig. 5.—Calculated satellite-trace shapes for the irregularities (a), (b), and (c) illustrated in Figure 4.

The range-spreading traces of set 1, which are resolved or partially resolved, also follow the main trace in shape. If off-vertical reflections from blobs or holes occur to produce range spreading then satellite-trace shapes similar to that of the main trace will not be expected in view of the frequency-spreading results given in Figure 5.

The evidence presented in this subsection suggests that the irregularities do not have the form of blobs or holes. Figure 2 of Booker (1961) shows the distorted nature of satellite traces resulting from a hole in the ionosphere produced by the transit of a missile.

*(c) Specular Reflection from Columns of Enhanced Ionization*

Aspect-sensitive reflections at frequencies greater than the critical frequency of the  $F_2$  layer are regularly observable (Peterson *et al.* 1955; Swenson 1964).

There seems little doubt that the irregularities responsible for these reflections are field-aligned columns of enhanced ionization. The observed ranges to these irregularities for azimuths slightly displaced from the direction of the magnetic pole strongly suggest this type of irregularity. It is possible that, for the frequencies which are normally reflected from the  $F_2$  layer, aspect-sensitive reflections occur after suitable refraction has turned the ray so that it is perpendicular to the magnetic field direction.

In a layer where the electron density varies linearly with height, in a vertical direction, calculations can be made for the ray paths through the layer for any particular angle of incidence. In these calculations the effect of the Earth's magnetic field has been neglected. For such a layer we can write  $N = \alpha^2 z$ , where  $z$  is the height measured from the base of the layer,  $N$  is the electron density content, and  $\alpha$  is a constant. For the particular model used here  $\alpha^2$  can be calculated. Also, since the square of the plasma frequency at any height is proportional to the electron density, we can write  $f_p^2 = K^2 N$ , where  $K$  is a known constant and  $f_p$  is the plasma frequency. For a particular angle of incidence of upgoing radiation,  $\theta_0$ , the horizontal distance  $D$  travelled by the ray before it reaches the ground again is given by

$$D = 4(f^2/\alpha^2 K^2) \sin \theta_0 \cos \theta_0 + 2h_0 \tan \theta_0,$$

where  $f$  is the operating frequency and  $h_0$  is the height of the base of the layer. The horizontal displacement of the position of the maximum height reached by the ray is therefore given by  $\frac{1}{2}D$ . An additional calculation of the maximum height in the layer,  $z_r$ , reached by this ray will give the precise position (point E in Fig. 6) in the layer for the maximum vertical excursion of the ray

$$z_r = (f^2 \cos^2 \theta_0) / \alpha^2 K^2.$$

The equations used in the foregoing discussion in this subsection are given by Kelso (1964). The path in the layer (HDEJ in Fig. 6) is a parabola and is given by

$$x = x_{\max}(1 - z^2/z_{\max}^2),$$

where  $x$  is the horizontal distance measured from point L in Figure 6 and  $z$  is the vertical displacement of the ray from the base of the layer HLJ. Using this relationship, enough points were determined to allow the ray path for any particular angle of incidence and operating frequency to be determined with reasonable accuracy. Figure 7 has been drawn to indicate some of the ray paths calculated in this subsection, for an angle of incidence in this case of  $20^\circ$ . Point D (Figs. 6 and 7) was determined by finding the position where the tangent to the curve was perpendicular to the direction of the magnetic field at Ellsworth ( $24^\circ$  from a vertical direction). The group path for the ray that travels a path AHD is given by the straight line AB (Fig. 6; see also Fig. 7) by Breit and Tuve's theorem (Budden 1961). Two cases are considered.

If the ray originates at point A (Fig. 6) and travels south in the magnetic meridian plane (southern hemisphere) to be reflected at perpendicular incidence with the field-aligned irregularity, the group path is given by AB (that is, AC-BC). If the ray starts at G (Fig. 6) and travels north in the magnetic meridian plane (southern hemisphere) for a similar reflection situation, the group path is given by AC+BC since Figure 6 is symmetrical about CL. In this way calculations were made for a

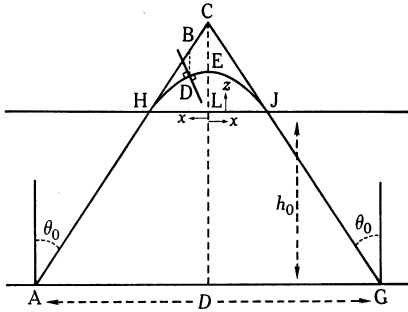


Fig. 6.—Illustration of a ray path through an ionosphere where the electron density varies linearly with height.

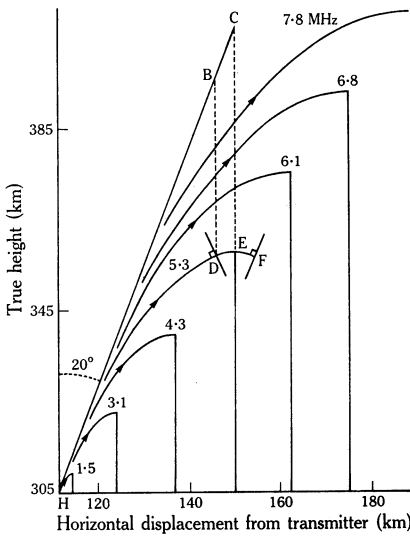


Fig. 7.—Ray paths for various frequencies through a "linear" ionosphere for an angle of incidence of 20°.

number of angles of incidence and of frequencies. It has been assumed that the proposed irregularities are capable of reflecting rays that are incident perpendicular to their orientation from any location in the layer. The maximum density of the model layer used restricted the frequencies that could be reflected in this manner. The model was calculated from the ionogram taken at Ellsworth at 0315 hr (local time), April 26, 1958. Figure 1(p) shows an ionogram taken 1 hr 20 min earlier than the one used for the model. It is similar in appearance. An  $N(h)$  analysis of the main trace of the ionogram taken at 0315 hr produced an electron density distribution given by the points in Figure 8. It will be seen that there is a linear variation of density from a base height of 305 km to a maximum for the layer of 410 km. The termination of the layer at 410 km was determined from the value of  $f_0F_2$  (7 MHz).

The group paths for signals arriving from the same directions in the magnetic meridian plane ( $10^\circ$ ,  $25^\circ$ ,  $35^\circ$ ,  $40^\circ$ , and  $45^\circ$  off-vertical) are shown by Figures 9(a) and 9(b) for the two cases described in the previous paragraph. Group-path positions

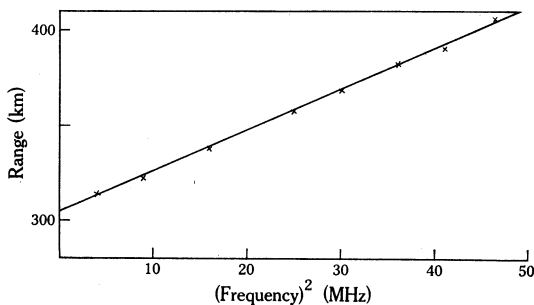


Fig. 8.—Electron density (proportional to frequency squared) profile calculated from the main trace of an Ellsworth ionogram at 0315 hr local time on April 26, 1958.

for a constant angle of incidence have been joined to give a trace over the range of frequencies which will be reflected for each angle. The plots have been made in this way for convenience in presentation. It does not imply that traces of this kind can

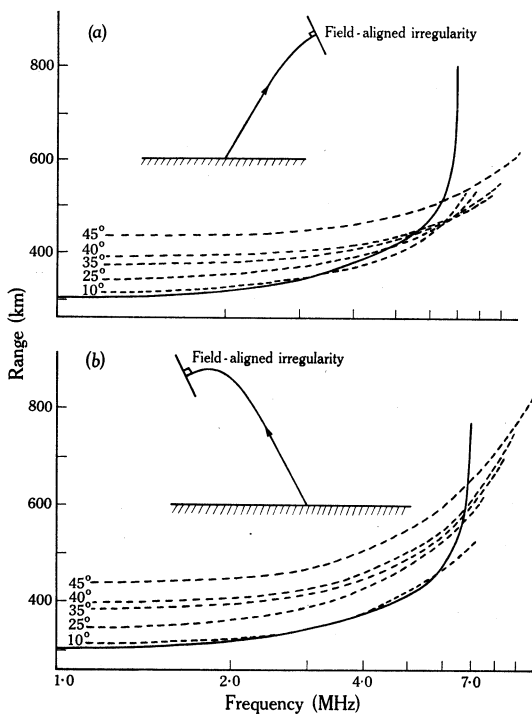


Fig. 9.—Calculated group ranges for

- (a) energy refracted in the model ionosphere and reflected at perpendicular incidence to field-aligned irregularities, and  
 (b) energy initially reflected from the layer at oblique incidence and subsequently reflected at perpendicular incidence to field-aligned irregularities.

be expected. If the ionosphere has field-aligned irregularities at evenly distributed positions, capable of reflecting all frequencies that are refracted to be perpendicular to the orientation of the irregularities, the plots in Figure 9 will give some indication

of the envelope of the spread- $F$  signals. It is only this envelope that should be compared with the observed characteristics of the phenomenon, particularly with those features observed in the ionogram shown by Figure 1( $p$ ). The results shown by Figure 9 were made assuming the same electron density distribution for horizontal displacements from the transmitter. The geometry is such that perpendicular incidence is possible for propagation outside the magnetic meridian plane. In this case each trace shown in Figure 9 can be imagined as widened in range to allow for these extra rays.

The predominant spreading in the ionogram used for the model is that described as set 1 in Section II. Set 2 is present but can only be detected by a careful inspection of the negative of this ionogram. Figure 1( $f$ ) is a high-gain record taken 2 hr 15 min earlier. It shows set 2 clearly. The results given in Figure 9, for propagation that is returned to the transmitter after being reflected at perpendicular incidence to the field-aligned irregularities, do not appear to represent the set 1 traces in Figure 1( $p$ ). For both Figures 9( $a$ ) and 9( $b$ ) the envelope of the satellite signals crosses the main trace giving spread- $F$  signals at frequencies higher than the critical frequency of the main trace. It is conceivable that set 2 of the spread- $F$  traces as illustrated in Figure 1( $f$ ) is related to the mode of propagation being investigated in this subsection, since the locations on the ionogram of the satellite signals are similar for both cases. This is discussed in Section IV.

#### (*d*) Waveguide Mechanisms

A number of authors have suggested that the radiation travels in ionospheric waveguides, oriented parallel to the magnetic field, before being returned to the transmitter site to form spread- $F$  signals on ionograms (see e.g. Klemperer 1963).

For this type of mechanism, one would expect the energy to be returned from directions centred on the direction of the magnetic field. Resolved traces extending over about the same frequency range as the main trace are sometimes observed with off-vertical angles between  $50^\circ$  and  $60^\circ$  (Bowman 1968*a*). It does not seem likely that in Antarctica, where the magnetic field direction approaches a direction perpendicular to the surface of the Earth, that these large off-vertical angles for the returning energy are consistent with the proposed waveguide mechanism.

When resolution of the satellite traces occurs in Antarctica, the horizontal distance in which the structure appears to repeat itself has been estimated at distances around 30 km (Fig. 2). This separation is too large to consider the propagation as being of the waveguide type. Further, it should be remembered that even when the traces appear diffuse this may result simply because the traces from these structures are a finite width due to the pulse width of transmissions.

It has been shown in Section II(*g*) that the phenomenon of spread- $F$  at mid latitudes and high latitudes is very similar, suggesting similar mechanisms in the production. At mid latitudes (Bowman 1968*b*) the azimuths of arrival of spread- $F$  signals are, on practically all occasions, well away (some tens of degrees) from the magnetic azimuth direction. This experimental observation is inconsistent with the concept of spread- $F$  signals returning after propagation in field-aligned waveguides.

*(e) Kinking of Contours of Equal Electron Density in the F<sub>2</sub> Region*

Since the phenomenon of spread-*F* seems to be the same at mid and high latitudes, a model similar to that used to explain mid latitude spread-*F* will be investigated here for observations at high latitudes. At times, records from topside sounders suggest reflections from structures that are somewhat similar to those given by this model (Muldrew 1963). The model will be based on some of the features of a particular ionogram showing spread-*F*. Figure 1(*k*) shows the ionogram that calculations from the model seek to reproduce with some degree of accuracy. The electron density distribution for a vertical direction from the station was the same as that calculated in Subsection (*b*) above. An ionogram taken 15 min before that shown in Figure 1(*k*) showed an enhanced trace with an off-vertical angle (determined from null displacements) consistent with propagation close to the magnetic field direction. An *N*(*h*) analysis of this enhanced trace therefore gave an electron density

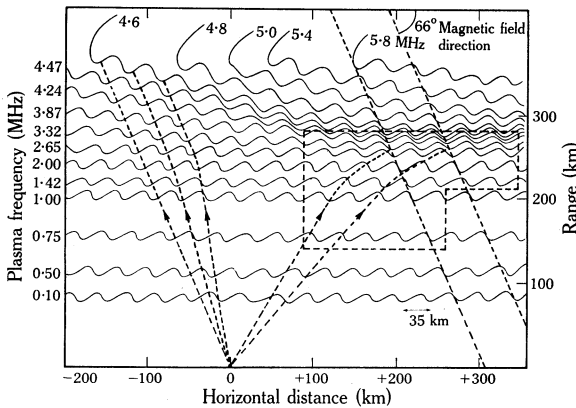


Fig. 10.—Model ionosphere involving kinking of ionization contours deduced by using information from Figure 1(*k*) (Ellsworth, 0900 hr local time, May 15, 1958). Some ray tracing is shown.

distribution for the proposed model in a direction  $24^\circ$  off-vertical. From these two distributions a model was built up with a horizontal gradient of  $f_0F_2$  which can be seen from Figure 10 to be continuous from one side of the transmitter to the other. A certain degree of resolution occurs on the ionogram shown in Figure 1(*k*) and the ionograms either side of it in time. From this an estimate of 35 km has been made for the horizontal distance in which the irregularity pattern repeats itself. Examination of Figure 10 will reveal the pattern of kinking that has been devised with the aid of the information derived from the ionograms. It is assumed that the cross section of the irregularities shown by Figure 10 is the same along a front several hundreds of kilometres in extent. The presence of the enhanced trace during the period suggests that the fronts extend in an east-west direction. However, this need not necessarily be precisely perpendicular to the plane containing the magnetic meridian. As in the model used for mid latitudes, the positions of kinks in the electron density contours have been made to change monotonically with height so that the irregularities have fronts sloping in directions close to the magnetic field direction.

Ray-tracing methods have been used to the left of the transmitter (see Fig. 10) to determine satellite traces which this structure might give. The effect of the magnetic

field has been neglected and Snell's law has been used in the ray tracing. It can be seen that a model such as this presents to radiation, travelling in the direction of the magnetic field, contours of equal ionization that are parallel to one another, similar to that encountered by radiation travelling vertically through a quiet horizontally stratified ionosphere. For this model, rays travelling in directions close to the magnetic field direction will produce echoes with greater signal strengths than from any other direction, because the kinking of the contours will be effective in dispersing radiation travelling in these other directions (vertical incidence included). Thus the model gives results consistent with the enhanced traces reported in Section II(d).

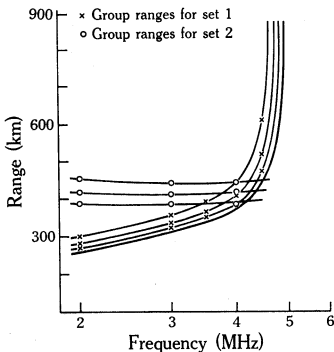


Fig. 11.—Reconstructed satellite traces using the model in Figure 10 for propagation to left and right of the transmitter.

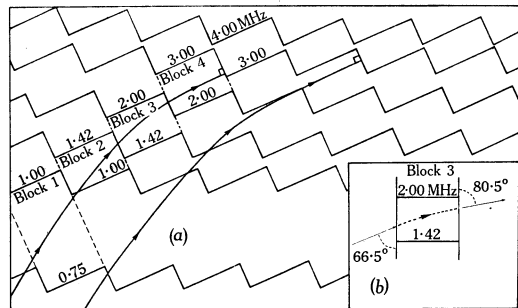


Fig. 12.—Idealized section (a) of the model in Figure 10 to allow calculations to the right of the transmitter; two ray paths are shown. (b) is an example showing the calculation for propagation in block 3.

The ray paths to the left of the transmitter which are drawn on Figure 10 are for a frequency of 4.58 MHz. Similar paths for other frequencies have been determined and the group paths calculated by evaluating  $\int 1/\mu ds$  along each path. Results are shown by the three satellite traces (Fig. 11) drawn through the calculated group paths indicated by crosses.

Because of the nature of the kinking used in the model it was more difficult to use Snell's law with any degree of accuracy for ray tracing to the right of the transmitter. Here a different method was used to get some indication of possible ray paths. The kinking was idealized so that the contours of equal electron density were alternatively perpendicular to the magnetic field lines and parallel to them. Figure 12 shows that portion of Figure 10 (enclosed by a dashed line) which has been treated in this way. The ionization has been divided into blocks. Within each block, the plasma frequencies terminating the upper and lower boundaries are determined from the model shown in Figure 10. Starting from the first block, the position of entry into the block and the direction of travel of radiation is known. It is assumed that between the upper and lower boundaries of each block the electron density varies linearly. Because of this assumption, by using equations given by Kelso (1964) for propagation in a linear layer (see Subsection (c) above) it has been possible to calculate for each block the position and direction of travel for radiation leaving the block. Calculations made from block to block eventually gave the angle between the direction of travel of the radiation and the field-aligned ionization contour that can be expected to reflect

the radiation for perpendicular incidence. Trial and error methods were used until an initial ray-path direction was found which terminated perpendicular to this electron density contour. Figure 12(a) shows two ray paths determined in this way. Figure 12(b) illustrates the calculation of the position and direction of travel of the emerging radiation for a particular block. Once the ray paths were determined the group path was calculated by using the expression  $\int 1/\mu ds$  along the path. Evaluation of this integral for the paths illustrated and also for paths at other frequencies has allowed the satellite traces shown in Figure 11 to be obtained (the open circles are the calculated points). It is realized that because, for the calculations just made, the nature of the kinking has been idealized the positions of these satellite traces will not be exact. Nevertheless, they do give some indication of the traces to be expected from the returning radiation that is initially propagated to the right of the transmitter in Figure 10.

The overall result shown by Figure 11, which was obtained by using ray-tracing methods in the model of Figure 10, appears to be promising. Two sets of traces can be expected. Further, the shapes of each set of satellite traces are consistent with observations (Section II(c)). The model also gives an explanation for the enhanced trace from a direction close to the magnetic field direction. The results from the model are also consistent with direction-of-arrival results (Bowman 1968a), which suggest that the reflection levels for the off-vertical satellite traces are approximately the same as the reflection levels for the same frequencies at vertical incidence.

It is possible to give a reasonably satisfactory explanation of the appearance of satellite traces that occur on multiple-hop main traces but that do not occur on the first-hop main trace (Section II(f)), by using a similar model with shallow oscillations. If it is assumed that the oscillation of the contours of equal electron density is so shallow that the maximum angle the orientation of the contours makes with the horizontal direction is  $15^\circ$ , the maximum possible ranges for ray paths for first-, second-, and third-hop satellite traces are shown in Figure 13(a). Retardation is neglected and a low frequency that would be reflected near the base of the layer is used. The details of these calculations are given below.

	Main Trace Range (km)	Maximum Possible Satellite Range (km)	Maximum Excess Range (km)
First hop	260	269	9
Second hop	520	560	40
Third hop	780	906	126

Because of the finite width of the traces, it is not possible to detect first-hop satellite traces (maximum excess range 9 km) with this model. It is possible for the second-hop and more likely for the third-hop satellite traces.

Figure 13(b) shows a model for the baseline of the layer incorporating a "shallow sine wave" variation with a maximum angle of  $15^\circ$  for the orientation of the baseline relative to the horizontal direction. Figure 13(b) seeks to show how this model can explain the resolved third-hop satellite traces shown in Figure 1(l) for a frequency of 2 MHz. The estimated ranges of 835, 860, and 885 km are relatively close to those observed (820, 860, and 880 km respectively). To get these ranges it has been necessary to use ray paths that leave and return to the transmitter with off-vertical angles of  $32^\circ$ ,  $38^\circ$ , and  $44^\circ$  respectively.

Using the system of nulls, the calculated off-vertical angles of arrival for these traces are  $30^\circ$ ,  $40^\circ$ , and  $43^\circ$  respectively. The spacing used between the oscillations, which could be considered as the wavelengths of the structures, is 45 km. Only specular reflections have been used. All factors considered, this seems to be a good model for the multiple-hop satellite traces.

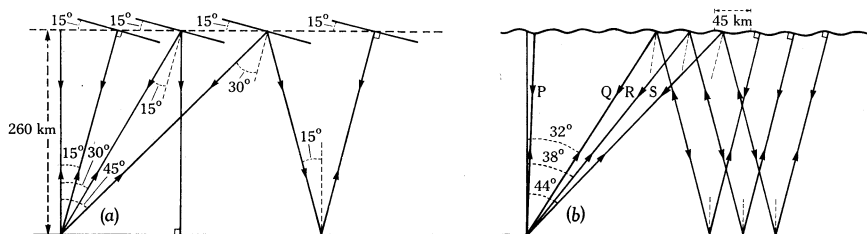


Fig. 13.—Illustrations of (a) maximum ray paths for first-, second-, and third-hop satellite traces for ionospheric irregularities with maximum slopes of  $15^\circ$ ; and (b) model and ray paths to explain third-hop satellite traces shown in Figure 1(l) (Ellsworth, 2200 hr local time, September 22, 1958):

	Angle Calculated from Null Position	Range (km)
P	—	258
Q	$30^\circ$	835
R	$40^\circ$	860
S	$43^\circ$	885

#### IV. DISCUSSION

Of all the models proposed in Section III the one that seems, at least, to be consistent with all the experimental evidence presented in Section II is that involving kinking of the ionization contours. Ray tracing in the model (Fig. 10) derived from the ionograms shown in Figure 1(k) has produced Figure 11, which has characteristics similar to those of this particular ionogram and to spread- $F$  ionograms generally.

The irregularities are probably the same type of phenomenon as the field-aligned sheets deduced by Muldrew (1963) from topside soundings, even though the orientation of the spread- $F$  fronts can presumably vary. Muldrew estimates the structure size at several kilometres, an order of magnitude less than the irregularity spacings obtained here by using satellite-trace spacings (Fig. 2).

The nature of any particular trace of set 2 on Figure 11 is similar to that for a trace expected for aspect-sensitive reflections from the same off-vertical angle (see Fig. 9(a)). It is possible that, instead of these traces resulting from reflection from sharply steeped contours of electron density, as was originally proposed, they are produced by aspect-sensitive reflections, after refraction in the layer, from field-aligned columns. In this case, the columns would be located at the positions in the layer where the kinking is most pronounced.

High latitude, mid latitude, and low latitude measurements (Klemperer 1963; Bowman 1960; Roy and Verma 1953) suggest specular reflection from relatively large-scale structures for spread- $F$  traces. The frequent occurrence of resolved traces on Antarctic records indicates structures of this type for polar regions.

Since radio-star scintillations were first recorded, associations have been found between these, or similar scintillations from Earth satellite transmissions, and spread- $F$  (see e.g. Klemperer 1963; Beynon and Jones 1964). There seems little doubt that a relationship exists between these phenomena. Early work has concentrated on the irregular fast fluctuations of radio-signal amplitude, which were ascribed to diffraction effects from an irregular screen (Hewish 1951). The irregularities producing the diffraction were later described as field-aligned columns of enhanced ionization (see e.g. Yeh and Swenson 1964). However, particularly as a result of the use of swept-frequency interferometers (Wild and Roberts 1956; Singleton 1964; Warwick 1964) scintillations of a different type have also been reported. Because these scintillations show systematic features that vary with frequency, workers were led to the suggestion that refraction effects from "lens-like", "prism-like", or "wave-like" irregularities in the  $F_2$  region with dimensions of the order of 10 km were responsible for these scintillations. The diffraction screen cannot be expected to give these frequency-dependent effects. Dagg (1957) reported particular types of scintillations at fixed frequency which he ascribed also to lens-like structures. Yeh and Swenson (1964) differentiated between the two types of scintillations, while Singleton (1964) has shown that the type of scintillation recorded seems to depend on the method of recording; he gives one example where both types are present simultaneously. Both Wild and Roberts (1956) and Singleton (1964) find associations between the second type of scintillations (associated with lens-like structures) and spread- $F$ .

Thus, the explanation of the association between scintillations and spread- $F$  does not appear to be as simple as at first thought. It does not seem likely that small-scale field-aligned irregularities are alone responsible for both scintillations and all types of spread- $F$ . Rather it appears from the foregoing that possibly two classes of ionospheric irregularities exist simultaneously. The same disturbance may be responsible for the creation of both the lens-like structures and the field-aligned columns. These irregularities would then be responsible for the different types of scintillations that are recorded.

In terms of the favoured results of this analysis the lens-like structure can be identified with the kinking of the ionization contours, and the columns of enhanced ionization may possibly exist at particular positions in this kinking structure. It has been suggested here that the traces most often seen in the spread- $F$  phenomenon (set 1) result from specular reflection from the relatively large-scale structure while possibly set 2 is produced by aspect-sensitive reflections from the field-aligned columns associated with the kinking.

## V. CONCLUSIONS

For reasons that have already been discussed, the model for the irregularities that produce spread- $F$ , which is favoured in this paper, consists of a simple kinking of the  $F_2$ -layer contours of equal electron density. This kinking produces quasi-sinusoidal shapes in these contours with wavelengths of some tens of kilometres. The position of the kinking in the layer is displaced monotonically with height in a way that is related to the orientation of the magnetic field (see Bowman 1960).

The orientation of the fronts along which the kinking occurs is not necessarily perpendicular to the magnetic-meridian plane since mid latitude results have shown that these fronts are often 30° or more away from this direction (Bowman 1960; Clarke 1965; Bowman 1968b). However, because of the frequent occurrence of the enhanced satellite trace on Antarctic ionograms it seems likely that the fronts here are often close to being magnetically east-west.

In the past, theoretical work on  $F_2$ -layer irregularities has concentrated on explaining local enhancements or reductions in electron density. If, as this paper suggests, kinking of the ionization contours plays a dominant role in the production of spread- $F$ , it may be profitable to investigate disturbances that might possibly explain this aspect of the phenomenon.

#### VI. ACKNOWLEDGMENTS

The author would like to thank Professor H. C. Webster, Dr. R. B. Penndorf, and Mr. G. F. Rourke for helpful assistance in the preparation of this paper. He is also grateful to Miss B. Willey, Miss E. Gistis, and Mr. S. H. Rosen, who made most of the calculations. The research was supported by the National Science Foundation under Contract NSF-C403.

#### VII. REFERENCES

- BEYNON, W. J. G., and JONES, E. S. O. (1964).—*J. atmos. terr. Phys.* **26**, 1175.  
 BOOKER, H. G. (1961).—*J. geophys. Res.* **66**, 1073.  
 BOWMAN, G. G. (1957).—M.Sc. Thesis, University of Queensland.  
 BOWMAN, G. G. (1960).—*Planet. Space Sci.* **2**, 133.  
 BOWMAN, G. G. (1968a).—*J. atmos. terr. Phys.* **30**, 1115.  
 BOWMAN, G. G. (1968b).—*J. atmos. terr. Phys.* **30**, 721.  
 BUDDEN, K. G. (1961).—"Radio Waves in the Ionosphere." pp. 186-7. (Cambridge Univ. Press.)  
 CLARKE, R. H. (1965).—M.Sc. Thesis, University of Queensland.  
 DAGG, M. (1957).—*J. atmos. terr. Phys.* **11**, 118.  
 HERMAN, J. R. (1966).—*Rev. Geophys.* **4**, 255.  
 HEWISH, A. (1951).—*Proc. R. Soc. A* **209**, 81.  
 KELSO, J. M. (1964).—"Radio Ray Propagation in the Ionosphere." Ch. 5. (McGraw-Hill: New York.)  
 KLEMPERER, W. K. (1963).—*J. geophys. Res.* **68**, 3191.  
 MULDREW, D. B. (1963).—*J. geophys. Res.* **68**, 5355.  
 PETERSON, A. M., VILLARD, O. G., JR., LEADABRAND, R. L., and GALLAGHER, P. B. (1955).—*J. geophys. Res.* **60**, 497.  
 PITTEWAY, M. L. V. (1962).—*J. geophys. Res.* **67**, 5107.  
 ROY, R., and VERMA, J. K. D. (1953).—*J. geophys. Res.* **58**, 473.  
 SATO, T., and ROURKE, G. F. (1964).—*J. geophys. Res.* **69**, 4591.  
 SHARP, G. W., CROTHER, T. J., and GILBRETH, C. W. (1964).—*Trans. Am. geophys. Un.* **45**, 87.  
 SINGLETON, D. G. (1964).—*J. Res. natn. Bur. Stand.* **68D**, 867.  
 SWENSON, E. M. (1964).—*Aust. J. Phys.* **17**, 490.  
 TITHERIDGE, J. E. (1966).—*Polar Rec.* **13**, 7.  
 VENTRICE, C. A., and SCHMERLING, E. R. (1958).—Penn. State Univ. Sci. Rep. No. 106.  
 WARREN, E. S. (1963).—*Nature, Lond.* **197**, 636.  
 WARWICK, J. W. (1964).—*J. Res. natn. Bur. Stand.* **68D**, 179.  
 WILD, J. P., and ROBERTS, J. A. (1956).—*J. atmos. terr. Phys.* **8**, 55.  
 YEH, K. C., and SWENSON, G. W., JR. (1964).—*J. Res. natn. Bur. Stand.* **68D**, 881.